Philosophical Magazine

ISSN: 1478-6435 (Print) 1478-6443 (Online) Journal homepage: http://www.tandfonline.com/loi/tphm20

A model for the initiation of reaction sites during the uranium–hydrogen reaction assuming enhanced hydrogen transport through thin areas of surface oxide

Joseph Glascott

To cite this article: Joseph Glascott (2014) A model for the initiation of reaction sites during the uranium–hydrogen reaction assuming enhanced hydrogen transport through thin areas of surface oxide, Philosophical Magazine, 94:3, 221-241, DOI: 10.1080/14786435.2013.852286

To link to this article: http://dx.doi.org/10.1080/14786435.2013.852286

Published online: 29 Oct 2013.

Submit your article to this journal

Article views: 136

View related articles

View Crossmark data

Citing articles: 11 View citing articles

Full Terms & Conditions of access and use can be found at
http://www.tandfonline.com/action/journalInformation?journalCode=tphm20

Download by: [The University of Manchester Library] **Date:** 22 September 2017, At: 03:21

Philosophical Magazine, 2014
Vol. 94, No. 3, 221–241, http://dx.doi.org/10.1080/14786435.2013.852286

Taylor & Francis
Taylor & Francis Group

A model for the initiation of reaction sites during the uranium–hydrogen reaction assuming enhanced hydrogen transport through thin areas of surface oxide

Joseph Glascott*

AWE, Aldermaston, Reading, Berkshire, UK

(*Received 7 June 2013; accepted 25 September 2013*)

A model for the initiation of hydride sites on uranium metal is described for conditions of constant hydrogen pressure. The model considers variations in hydrogen permeation through the surface oxide film due to intrinsic variations in the oxide thickness. It is proposed that thin areas of surface oxide favour enhanced hydrogen permeation through the oxide and lead to the more rapid initiation of hydride sites. The time and spatial dependence of the hydrogen concentration field in the metal underlying thin areas of oxide is calculated in terms of the local oxide film thickness, the hydrogen diffusion coefficients in the oxide and metal and the hydrogen concentration in the oxide at the gas–oxide interface. The time to precipitate hydride at any location is calculated by assuming that precipitation occurs once the hydrogen concentration in the metal attains the terminal solubility limit of the metal at the prevalent temperature. The model is compatible with the reported temperature and pressure dependence of the hydride induction time. The model can also explain observations such as precipitation of hydride at or beneath the oxide–metal interface and the arrested growth of hydride sites. Finally, an expression is derived for the number of hydride sites initiated on an entire sample surface in any given time by assuming a Gaussian oxide film thickness distribution over the entire sample surface.

Keywords: uranium; hydriding; model; initiation

Downloaded by [The University of Manchester Library] at 03:21 22 September 2017

1. Introduction

Uranium metal is used as a fuel in some nuclear reactors (e.g. Magnox reactors). Owing to its high reactivity with both oxygen and water, and the fact that reaction of the metal with water can generate hydrogen which also can react rapidly with the metal, unwanted corrosion of the metal is an ever-present concern. Additionally, even after their use, fuel rods containing uranium metal pellets frequently corrode in cooling pools allowing water to access the uranium; excessively corroded fuel rods present serious challenges to the safe treatment and storage of the arising radioactive waste, and the generation of pyrophoric uranium hydride is a particular concern. Consequently, if the extent of uranium corrosion likely to be experienced in any given scenario is to be

*Email: joe.glascott@awe.co.uk

© 2013 Crown Copyright

quantified, there is a need to better understand the kinetics and mechanisms of all relevant corrosion reactions but particularly the hydriding reaction.

Now although clean uranium metal reacts rapidly with pure hydrogen over its entire surface [1], more generally hydride attack occurs initially in a localized manner. Localized attack of the metal is attributed to the existence of a semi-protective surface oxide film on the metal [2–4]. Previous models of hydride initiation [5,6] generally invoke the natural proposal that hydrogen species must diffuse through this oxide film before hydride precipitation can occur in the metal at any particular location. Such hydride initiation models are therefore at least qualitatively compatible with the general observations that increase in temperature or hydrogen pressure lead to a more rapid rate of hydride site initiation [5], whereas increases in mean oxide thickness lead to a less reactive surface [3,7]. Localized attack implies localized variation in some relevant oxide characteristic. If enhanced hydrogen transport through the surface oxide film is associated with the initiation of hydride sites in the metal, several different oxide features may be proposed which could be understood to give rise to such enhanced hydrogen flow. Figure 1 illustrates typical features which might be expected to be characteristic of a thin oxide film developed on a uranium metal surface. Firstly, oxide films on many metals initially tend to grow at different rates on the differently orientated metal grains [8,9], and so, it might be expected that the oxide thickness would vary from metal grain to metal grain. Qualitatively, it may be said that any variation in oxide thickness over the different uranium metal grains would be reflected in localized variations in hydrogen flow through the oxide film; also, hydrogen permeation through the oxide film on any particular metal grain would give rise to an area source of hydrogen flow into the underlying metal. Any pores in the oxide film would also give rise to an area source of hydrogen flow into the underlying metal although in this case the area source might be so small that it may be regarded as a point source. A line defect in the surface oxide film (e.g. an edge dislocation), from the gas–oxide interface to the metal-oxide interface, would give rise to a true point source on the metal surface. Other

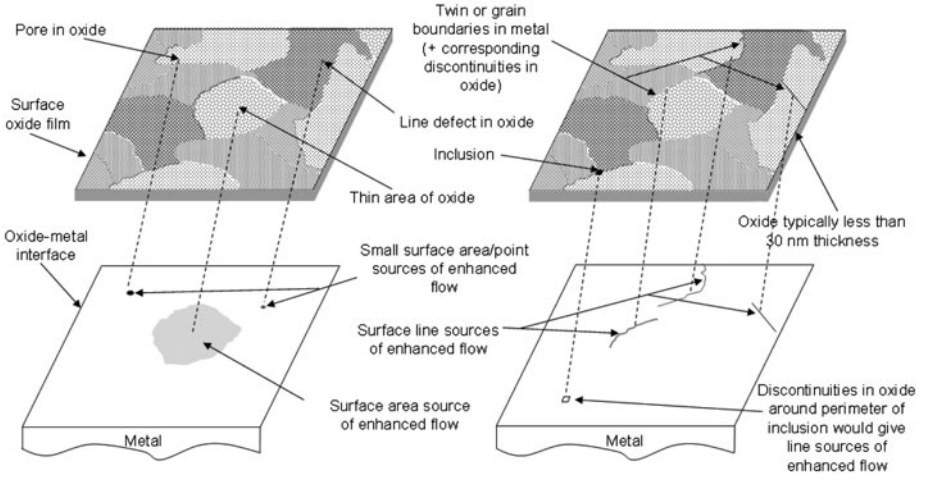

Figure 1. Illustration of various features of surface oxide film on uranium and how they may influence hydrogen access to the underlying metal.

Downloaded by [The University of Manchester Library] at 03:21 22 September 2017

principal features of the oxide film which might facilitate more rapid hydrogen transport to the metal are linear discontinuities in the oxide film associated with underlying metal grain or twin boundaries [10,11]. Although not all such linear oxide discontinuities may be fast diffusion paths for hydrogen, where these oxide discontinuities intersect the metal surface they would give rise to line sources of hydrogen flow into the metal. Finally, the boundary between the surface oxide film and inclusions in the metal which are present at the metal surface may also be expected to have different hydrogen transport characteristics than areas of oxide away from such features. For example, any temperature variations could lead to the development of microscopic gaps between a surface inclusion and the immediately adjacent oxide film due to the different thermal expansion coefficients of the metal and inclusion (usually carbide).

The above discussion proposes that the oxide film developed on uranium metal, although nominally conferring protection to the metal from hydrogen attack, contains numerous types of feature which may be more permeable to hydrogen, and at which locations hydride attack may occur preferentially. In order to compare experimental hydriding data with that expected from hydrogen transport through the oxide via any of the proposed surface features, however, it is necessary to examine mathematically the time and spatial dependence of the hydrogen concentration field developed in the metal in the region of such oxide/surface features. This paper is concerned with calculating the hydrogen concentration field in the metal for area sources associated with thin areas of surface oxide. This paper is also limited to conditions of constant hydrogen pressure. Surface line sources associated with linear discontinuities in the oxide film will be addressed in a later paper [12].

2. The model

2.1. *Model assumptions and system description*

This model of uranium hydride initiation is based on the proposal that if the oxide film is regarded as a hydrogen diffusion barrier then thin areas of oxide may lead to hydride attack of the underlying metal at earlier times compared with hydride attack occurring at later times elsewhere where the oxide is thicker. Like a model of uranium hydride initiation developed earlier [5], it is also assumed that the oxide film thickness distribution may be approximated to a Gaussian distribution. Unlike that previous model of hydride initiation, however, this model assumes that hydride will be initiated in the metal not when a given amount of hydrogen (per unit area) has diffused through any thin region of the oxide film but when the hydrogen concentration at any point in the metal just exceeds the terminal hydrogen solubility limit of the metal (C_{HS}) at the prevalent temperature. This model therefore takes into account the hydrogen transport properties of the metal as well as those of the surface oxide film. Except in declared cases, this model generally assumes that the metal is isotropic and therefore has uniform hydrogen solubility and uniform hydrogen diffusion coefficient (D_M) throughout its bulk. Also, we assume uniform oxide stoichiometry. Finally, we assume that at time zero (i.e. the time at which the metal is first exposed to hydrogen), the hydrogen concentration at any point x, y, z in the metal, $C_{H(x,y,z,0)}$, is also zero (where the origin of our coordinate system 0, 0, 0 is at the centre of the considered thin (and assumed circular) area of oxide film just adjacent to the oxide–metal interface – see Figure 2). As

Downloaded by [The University of Manchester Library] at 03:21 22 September 2017

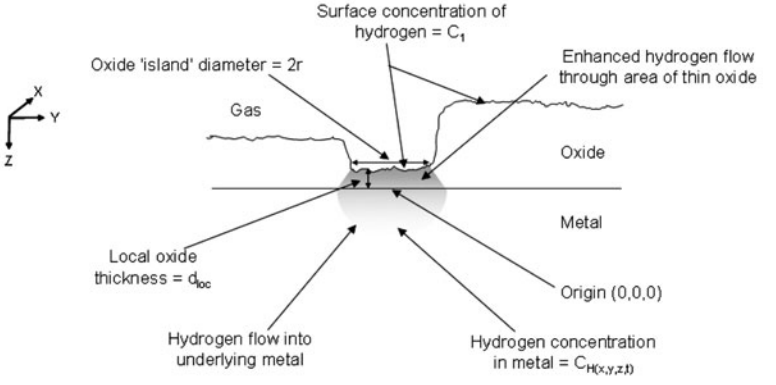

Figure 2. Schematic of variable thickness oxide film on metal where it is assumed that there will be more rapid hydrogen transport through thin oxide areas.

our presumed oxide thickness distribution on any polycrystalline sample surface is associated with different rates of prior oxide growth on the differently orientated metal grains, the diameter of each oxide area element, $2r$, is the same as the average metal grain diameter.

In order to derive an expression for the hydride initiation time in the region of a locally thin region of surface oxide, we must calculate the time and spatial dependence of the hydrogen concentration field in the metal. Here, no attempt is made to derive an expression fully describing the time and spatial dependence of the hydrogen concentration in the complete oxide and metal system. Instead, consideration is given to the hydrogen flow through the oxide, and the magnitude of this flow is then used to calculate the time and spatial dependence of the hydrogen concentration in the metal alone. Provided that certain model assumptions are complied with, this strategy is valid and fulfils our aims but avoids difficulties associated with defining the hydrogen concentration across the oxide–metal interface. Clearly, if this calculation is to be quantitative, consideration must be given to the magnitudes of the solubility and diffusion coefficient of hydrogen in uranium dioxide as these parameters determine the magnitude of the hydrogen flow. Additionally, this model relies on the assumption that the hydrogen flow through any thin region of oxide rapidly attains some near-constant value. To support this assumption, it is necessary to consider the hydrogen transport properties of uranium dioxide. Unfortunately, there have been only a limited number of studies examining the solubility and transport of hydrogen in uranium dioxide and not all of these data are consistent. A thorough review of this work will be presented in a later paper [13] where the model presented here is compared with uranium hydriding data over a wide range of temperatures and pressures. However, from the works of both Wheeler [14] and Aratono et al. [15], it would appear that hydrogen transport in uranium dioxide is fairly rapid, even at low temperatures. Using a hydrogen infusion/outgassing method, Wheeler measured the solubility and diffusion coefficient of hydrogen in single crystal UO_2 over the temperature range 500–1000 °C. Although Wheeler's measurements of hydrogen solubility were somewhat irreproducible from experiment to experiment, he obtained good reproducibility in his evaluations of the hydrogen

Downloaded by [The University of Manchester Library] at 03:21 22 September 2017

diffusion coefficient in the oxide, D_o, and his data fitted the relationship $D_o = 3.7 \times 10^{-2}$ Exp $(-60\,\mathrm{kJ\,mol^{-1}}/RT)$ $\mathrm{cm^2\,s^{-1}}$. Diffusion data obtained by Aratono et al. [15] fitted the relationship; $D_o = 1.5 \times 10^{-1}$ Exp $(-76\,\mathrm{kJ\,mol^{-1}}/RT)$ $\mathrm{cm^2\,s^{-1}}$. For the different thermal infusion studies, the fact that Wheeler, making use of single crystal UO_2, measured a similar diffusion coefficient of hydrogen in the oxide to that found by Aratono et al., who made use of a polycrystal, suggests that lattice rather than grain boundary diffusion in the oxide dominates its hydrogen permeability characteristics. Extrapolation of this data to lower temperatures more pertinent to the long-term storage of uranium metal suggests that even at say 30 °C the diffusion coefficient of hydrogen in uranium dioxide is in the region of 10^{-14}–10^{-12} $\mathrm{cm^2\,s^{-1}}$. Further considering the hydrogen solubility in uranium dioxide, measurements carried out by Sherman and Olander [16], although not in full agreement with the measurements of Wheeler [14], indicate that lattice hydrogen solubility in stoichiometric UO_2 is very small and approximately proportional to the square root of pressure.

Although there are clear inconsistencies in some of the reported data, the works of Wheeler, Aratono et al. and Sherman and Olander indicate that hydrogen species mobility in UO_2 is rapid, even at low temperatures, even though the amount dissolving at normal temperatures and pressures may be exceedingly small and highly dependent on the stoichiometry of the oxide. This conclusion allows us to comment on the interaction of hydrogen gas with a thin oxide film on a uranium metal surface and thereby calculate the developed hydrogen concentration profile in the metal as a function of time.

From the above studies [14–16], it may be proposed that when uranium metal bearing a thin oxide film (say <50 nm mean thickness) is exposed to hydrogen gas, the hydrogen flow through any thin region of oxide film will rapidly attain some near-constant value, even if the magnitude of that flow may be exceedingly small. This conclusion arises from a consideration of the flow of diffusant through a thin film (see Crank [17]) where the concentrations of diffusant in the opposing faces of the film, thickness d, are held at some constant values (C_1 and C_2). The driving force for diffusion (diffusion coefficient D) through the thin film is the concentration gradient across the film $(C_1 - C_2)/d$ and, if C_2 is always small compared with C_1, a near-constant flow of diffusant through the film is established in a time comparable with $d^2/6D$. Thus, if the uranium metal acts as an efficient solvent for hydrogen (compared with the oxide), readily transporting hydrogen away from the oxide–metal interface, and if C_{HS} is small compared with C_1, then for all times prior to hydride initiation beneath some locally thin region of oxide film the hydrogen flow through that region of oxide will be near-constant and approximately equal to $C_1 D_o/d$. A further assumption of this model is that there is no significant time delay (compared with any calculated hydride initiation time) between exposure to the hydrogen gas and the concentration of hydrogen in the oxide at the oxide surface, C_1, attaining some constant value related to, but not necessarily directly proportional to, the applied pressure. Additionally, it is assumed that the time required for the necessary atomic re-arrangement accompanying the transformation of hydrogen-saturated metal to uranium hydride [18] is negligible compared with the time required for the hydrogen concentration in the metal to attain the terminal solubility limit, which is determined by diffusion processes. That atomic re-arrangement accompanying hydride formation is rapid is evident from the work of Schulze [1] who observed no significant time delay between the exposure of his clean sample of uranium to deuterium gas and the formation of deuteride.

Downloaded by [The University of Manchester Library] at 03:21 22 September 2017

Downloaded by [The University of Manchester Library] at 03:21 22 September 2017

Lastly, we may note that our presumption is that hydrogen species (atomic) diffuse through the oxide lattice. However, this model would still be applicable if the hydrogen species diffused via the oxide grain boundaries provided that the oxide was microcrystalline throughout its depth (because this mode of transport through any thin area of oxide would still give an area source of hydrogen flow into the metal). The only necessary change to the model for the case of grain boundary diffusion of hydrogen species is to replace the hydrogen lattice diffusion coefficient with an 'effective' diffusion coefficient (a simple function of the true grain boundary diffusion coefficient of the hydrogen species, the grain boundary width and the oxide crystallite size).

For any considered locally thin region of oxide, therefore, the hydrogen flow through that portion of oxide will attain some near-constant value in a short time and this flow of hydrogen through the oxide and into the metal will lead to the development of a time-dependent concentration field in the underlying metal (Figure 2). Our problem of calculating the form of this hydrogen concentration field is equivalent to calculating the temperature rise in a semi-infinite solid in the region of a finite-area surface heat source of constant flow per unit area. A solution to this problem has been obtained by Carslaw and Jaeger [19, p. 264] and could be transformed from heat/temperature units to mass/concentration units. However, it is beneficial to derive the solution we require here because (i) an intermediate expression in this derivation may be used as the starting point in deriving solutions for C_H in the metal for cases where we have not constant but variable hydrogen gas pressure (to be published in a later paper) and (ii) this same intermediate expression is useful in allowing us to judge the effect on our calculated C_H due to hydrogen transport through thicker regions of oxide neighbouring our considered localized thin region of oxide.

2.2. *Calculation of the hydrogen concentration in the metal*

The starting point for calculating the time dependence of the hydrogen concentration in the metal beneath our assumed circular (radius r) finite area, constant flow hydrogen

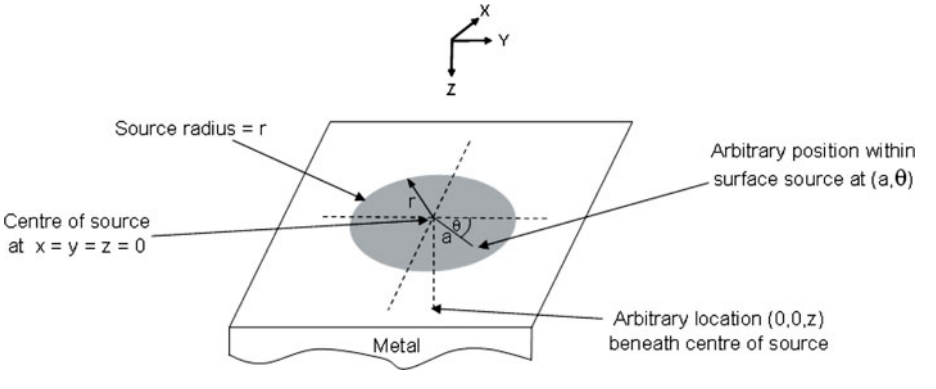

Figure 3. Diagram showing circular area source of hydrogen flow into the metal associated with a locally thin area of surface oxide. The origin of our coordinate system is at the centre of our source. Our aim is to calculate the time dependence of the hydrogen concentration in the metal at any distance, z, beneath the centre of the source.

source (see Figure 3), is the solution for the concentration of diffusant in a semi-infinite body for the case of an instantaneous point source (mass m) on the surface of the body. If the hydrogen concentration at $t = 0$ is zero in the metal at all x, y and z, then the concentration of hydrogen at any point x, y, z and at time, t, due to an instantaneous point source of hydrogen (mass m) released at $x = y = z = 0$ at time $t = 0$ is (see Crank [17] p. 29):

$$C_{H(x,y,z,t)} = \frac{m}{4(\pi D_M t)^{3/2}} \mathrm{Exp}\left(-\frac{x^2+y^2+z^2}{4D_M t}\right) \tag{1}$$

To calculate $C_{H(x,y,z,t)}$ in the metal due to our finite area and constant source, we simply need to integrate this expression with respect to the size of our area source (to give the solution for $C_{H(x,y,z,t)}$ for the case of an instantaneous surface area source) and then time (to obtain the solution for a continuous surface area source). Therefore, using the cylindrical coordinate system to define positions within our surface source, consider an instantaneous circular finite area source (radius = r) centred about the origin $(0, 0, 0)$ on the surface of the semi-infinite body. Confining ourselves to consider only points in the semi-infinite metal directly beneath the centre of the circular surface source, the concentration of hydrogen $C_{H(0,0,z,t)}$ at time t and at distance z directly beneath the centre of the source due to the instantaneous deposition of mass m of hydrogen at the location (a, θ) on the surface at time $t = t$ is given by:

$$C_{H(0,0,z,t)} = \frac{m}{4(\pi D_M t)^{3/2}} \mathrm{Exp}\left(-\frac{(a^2+z^2)}{4D_M t}\right)$$

Now for a circular source, radius r, centred on (0,0,0), the size of any small elemental area within that source (bounded by a and $a + \delta a$ and θ and $\theta + \delta\theta$) is equal to $a.\delta a.\delta\theta$. So, if we now consider the concentration of hydrogen in the underlying semi-infinite body at time t due to an instantaneous circular source of radius r on the surface of the body and where the mass deposited is m_a g per unit area, the mass of hydrogen deposited over any small elemental area is equal to the product $m_a.a.\delta a.\delta\theta$, and so, the concentration of hydrogen at $(0, 0, z, t)$ due to the integrated effect of the entire hydrogen mass deposited over the circular source on the body surface instantaneously at time $t = 0$ is:

$$C_{H(0,0,z,t)} = \frac{m_a}{4(\pi D_M t)^{3/2}} \int_0^{2\pi} \int_0^r a \ \mathrm{Exp}\left[-\frac{(a^2+z^2)}{4D_M t}\right] da d\theta \tag{2}$$

Integrating first with respect to a gives:

$$C_{H(0,0,z,t)} = \frac{m_a \mathrm{Exp}\left[-\frac{z^2}{4D_M t}\right]}{4(\pi D_M t)^{3/2}} \int_0^{2\pi} 2D_M t\left[1 - \mathrm{Exp}\left[-\frac{r^2}{4D_M t}\right]\right] d\theta$$

Now integrating then with respect to θ gives:

$$C_{H(0,0,z,t)} = \frac{m_a \mathrm{Exp}\left[-\frac{z^2}{4D_M t}\right]}{(\pi D_M t)^{1/2}} \left[1 - \mathrm{Exp}\left[-\frac{r^2}{4D_M t}\right]\right] \tag{3}$$

Downloaded by [The University of Manchester Library] at 03:21 22 September 2017

This expression gives the concentration of hydrogen in the underlying semi-infinite body at time t due to an instantaneous circular source of radius r on the surface of the body and where the mass deposited, at time $t = 0$, is m_a g per unit area. If we now consider a continuous and constant source which emits mass $dt'.m'_a$ g cm^{-2} of hydrogen during any finite time interval from $t = t'$ to $t = t' + dt'$ from time $t = 0$ then the concentration at any point $(0, 0, z)$ directly beneath the centre of the surface area source at time $t = t$ is, referring to Equation (3):

$$C_{H(0,0,z,t)} = \frac{m'_a}{(\pi D_M)^{1/2}} \int_0^t \frac{1}{(t-t')^{1/2}} \mathrm{Exp}\left[-\frac{z^2}{4D_M(t-t')}\right] - \frac{1}{(t-t')^{1/2}} \mathrm{Exp}\left[-\frac{(r^2+z^2)}{4D_M(t-t')}\right] dt' \tag{4}$$

Consider just the first part of this integral:

$$I_1 = \frac{m'_a}{(\pi D_M)^{1/2}} \int_0^t \frac{1}{(t-t')^{1/2}} \mathrm{Exp}\left[-\frac{z^2}{4D_M(t-t')}\right] dt'$$

If we make the substitution, $\Phi = z/(4\ D_M\ (t-t'))^{1/2}$ then this integral transforms to:

$$I_1 = \frac{m'_a}{(\pi D_M)^{1/2}} \int_{z/(4D_M t)^{1/2}}^{\infty} \frac{z}{\Phi^2 (D_M)^{1/2}} \mathrm{Exp}\left[-\Phi^2\right] d\Phi$$

Integrating this by parts gives:

$$I_1 = \frac{2m'_a(t)^{1/2}}{(D_M)^{1/2}} \left[\frac{1}{(\pi)^{1/2}} \mathrm{Exp}\left[-\frac{z^2}{4D_M t}\right] - \frac{z}{(4D_M t)^{1/2}} \mathrm{Erfc}\left[\frac{z}{(4D_M t)^{1/2}}\right]\right]$$

or

$$I_1 = \frac{2m'_a(t)^{1/2}}{(D_M)^{1/2}} \left[i\mathrm{Erfc}\left[\frac{z}{(4D_M t)^{1/2}}\right]\right] \tag{5}$$

By a similar process, the second component of the original integration can also be solved, that is,

$$I_2 = -\frac{m'_a}{(\pi D_M)^{1/2}} \int_0^t \frac{1}{(t-t')^{1/2}} \mathrm{Exp}\left[-\frac{(r^2+z^2)}{4D_M(t-t')}\right] dt'$$

becomes

$$I_2 = -\frac{2m'_a(t)^{1/2}}{(D_M)^{1/2}} \left[i\mathrm{Erfc}\left[\frac{(r^2+z^2)^{1/2}}{(4D_M t)^{1/2}}\right]\right]$$

Thus, the required concentration at $(0, 0, z, t)$ being the sum of these two components (see original integration) is given by:

$$C_{H(0,0,z,t)} = \frac{2m'_a(t)^{1/2}}{(D_M)^{1/2}} \left[i\mathrm{Erfc}\left[\frac{z}{(4D_M t)^{1/2}}\right] - i\mathrm{Erfc}\left[\frac{(r^2+z^2)^{1/2}}{(4D_M t)^{1/2}}\right]\right]$$

Downloaded by [The University of Manchester Library] at 03:21 22 September 2017

Lastly, if we replace the term m'_a representing amount of hydrogen transported through unit area of our considered locally thin region of oxide film (thickness d_{loc}) per unit time with the appropriate terms relating to this assumed near-constant hydrogen flow through the oxide then we have:

$$C_{H(0,0,z,t)} = \frac{2C_1\ D_o(t)^{1/2}}{d_{loc}(D_M)^{1/2}}\left[i\mathrm{Erfc}\left[\frac{z}{(4D_Mt)^{1/2}}\right] - i\mathrm{Erfc}\left[\frac{(r^2+z^2)^{1/2}}{(4D_Mt)^{1/2}}\right]\right] \quad (6)$$

So, considering only hydrogen transport into the metal through a locally thin circular (radius r) region of surface oxide film, Equation (6) gives the value of the hydrogen concentration in the underlying metal at any depth z directly beneath the centre of that assumed circular thin region of oxide.

3. Model characteristics

3.1. *Effects influencing locations and initiation times of individual hydride sites*

Having derived the expression (Equation (6)) describing the time and spatial dependence of the hydrogen concentration in the metal beneath a localized region of thin oxide film, consider now the characteristics of this expression to understand how the various system and operational parameters influence hydride initiation times. Firstly, it is clear that for any value of local oxide film thickness, d_{loc}, and at any time, t, the hydrogen concentration at any depth into the metal beneath the centre of the thin region of oxide is directly proportional to the steady-state hydrogen flow ($=D_oC_1/d_{loc}$) through unit area of that particular region of the oxide film. Thus, at any given temperature, hydrogen pressure and time, the hydrogen concentration at any particular depth into the metal will be greatest where the oxide film is thinnest. Further, Figure 4 shows the time

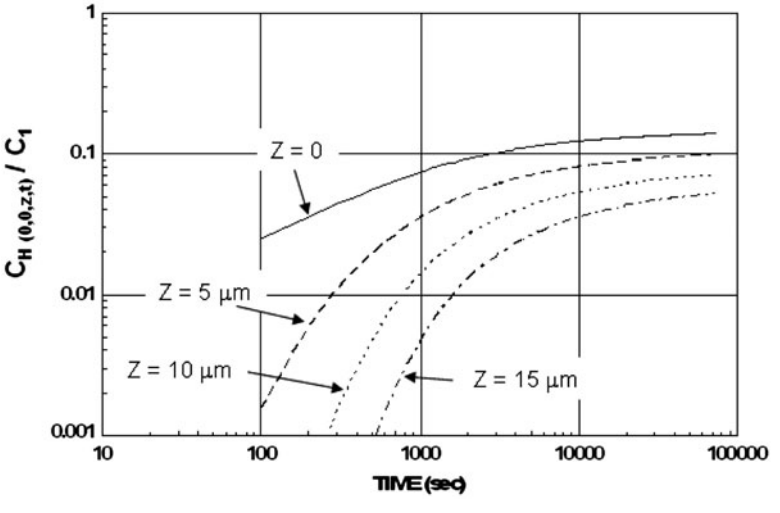

Figure 4. Time dependence of the calculated hydrogen concentration in the metal at three different values of distance, z, beneath the centre of a locally thin circular area of oxide (for $D_M = 5 \times 10^{-10}$ cm^2 s^{-1}, $D_o = 10^{-13}$ cm^2 s^{-1}, $d_{loc} = 20$ nm and $r = 15$ µm).

Downloaded by [The University of Manchester Library] at 03:21 22 September 2017

Downloaded by [The University of Manchester Library] at 03:21 22 September 2017

dependence of $C_{H(0,0,z,t)}$ for values of z of 0, 5, 10 and 15 μm. In passing, it may be noted that in all example calculation presented here, the values of the various model parameters (r, D_o, D_M, etc.) are those expected for typical uranium samples at about 30 °C based on extrapolation of diffusion data cited in the quoted references. Figure 4 shows that at any given time (and for any value of d_{loc}), the hydrogen concentration in the metal is greatest at $z = 0$ (i.e. at the oxide–metal interface). Therefore, for any thin region of surface oxide film, the hydrogen concentration profile in the metal beneath the oxide is such that the hydrogen solubility limit of the metal will be exceeded first immediately adjacent to the oxide–metal interface. Therefore, according to this model, hydride precipitation should occur first in the metal just adjacent to the oxide–metal interface at the centre of any considered thin region of oxide film. The precipitation of hydride may not immediately disrupt the oxide film but, due to the volume expansion accompanying the transformation of uranium metal to uranium hydride, this should probably occur once the size of the incipient hydride spot is comparable to the oxide thickness. Once the oxide film has been disrupted by the small growing hydride spot, thereafter its growth will not be controlled by diffusion of hydrogen species through the oxide film. Figure 4 also shows that, for any value of z, the hydrogen concentration in the metal continually increases with time but it approaches some asymptotic value. From Equation (6) and for $z = 0$, $C_{H(0,0,0,t)}$ is given by Equation (7).

$$C_{H(0,0,0,t)} = \frac{2\ C_1 D_o (t)^{1/2}}{d_{loc} (D_M)^{1/2}} \left[\frac{1}{(\pi)^{1/2}} - i\mathrm{Erfc}\left[\frac{r}{(4D_M t)^{1/2}} \right] \right] \tag{7}$$

Also, it can be seen that at early times where $t << r^2/4D_M$ (such that $i\mathrm{Erfc}(r/(4D_M{\cdot}t)^{½}) << 1/(\pi)^{½}$) then $C_{H(0,0,0,t)}$ initially increases as the square root of time. At such early times, to a good approximation $C_{H(0,0,0,t)}$ is then given by Equation (8).

$$C_{H(0,0,0,t)} \approx \frac{2C_1 D_o (t)^{1/2}}{d_{loc} (\pi D_M)^{1/2}} \quad \text{(at early times)} \tag{8}$$

Lastly, we can consider how rapidly $C_{H(0,0,0,t)}$ initially increases with time (at $z = 0$) by differentiating Equation (7) to obtain an expression for $\mathrm{d}(C_{H(0,0,0,t)})/\mathrm{d}t$:

$$\frac{d(C_{H(0,0,0,t)})}{d(t)} = \frac{C_1 D_o}{d_{loc} (\pi D_M t)^{1/2}} \left[1 - \mathrm{Exp}\left(-\frac{r^2}{4D_M t} \right) \right] \tag{9}$$

From this equation, it can be seen that $C_{H(0,0,0,t)}$ increases most rapidly where d_{loc} is least.

At $z = 0$, the magnitude of the asymptotic value of $C_{H(0,0,0,t)}$ attained at $t = \infty$ is not immediately obvious as, at such times, the term outside of the brackets in Equation (7) approaches infinity whilst the term inside the brackets would seem to approach zero. However, writing $i\mathrm{Erfc}(r/(4D_M{\cdot}t)^{½})$ as $((1/\pi)^{½}.\mathrm{Exp}(-r^2/(4D_M{\cdot}t)) - (r/(4D_M{\cdot}t)^{½}).\mathrm{Erfc}((r/(4D_M{\cdot}t)^{½})))$ and recognizing that the terms $\mathrm{Exp}(-r^2/(4D_M{\cdot}t))$ and $\mathrm{Erfc}((r/(4D_M{\cdot}t)^{½}))$ both tend to 1 as t approaches infinity then it is clear that $i\mathrm{Erfc}(r/(4D_M{\cdot}t)^{½})$ approximates to $((1/\pi)^{½} - (r/(4D_M{\cdot}t)^{½}))$ as t approaches infinity and so the value of $((1/\pi)^{½} - i\mathrm{Erfc}((r/(4D_M{\cdot}t)^{½})))$ just tends to $(r/(4D_M{\cdot}t)^{½})$ as t approaches infinity. Hence, as t approaches

Downloaded by [The University of Manchester Library] at 03:21 22 September 2017

infinity, the value of $C_{H(0,0,0,t)}$ approaches $D_o.C_1.r/d_{loc}.D_M$. Thus, according to Equation (7), even though there is a constant flow of hydrogen through the oxide film at any particular location, the (maximum) hydrogen concentration in the metal just adjacent to the oxide–metal interface does not increase indefinitely; simultaneous hydrogen diffusion away from this interface into the bulk of the metal causes the hydrogen concentration to reach some equilibrium value. Consequently, at some locations and depending on the value of local oxide film thickness, the maximum attained value of hydrogen concentration in the metal may be less than the hydrogen solubility limit of the metal. In such cases, hydride precipitation will never occur at this location. This point is illustrated by the plots shown in Figure 5. For each value of local oxide film thickness, the maximum hydrogen concentration in the metal immediately adjacent to the oxide–metal interface increases initially as the square root of time before eventually approaching the limiting value of $D_o.C_1.r/d_{loc}.D_M$, as discussed above. Thus, the maximum hydrogen concentration in the metal beneath any thin region of oxide film (at $z = 0$) is inversely proportional to d_{loc}, and this has the consequence that, for any particular value of terminal hydrogen solubility in the metal, there will be a critical value of local oxide film thickness, d_{crit}, above which hydride precipitation will not occur. Since the maximum attained hydrogen concentration in the metal is equal to $D_o.C_1.r/d_{loc}.D_M$, then d_{crit} (the local oxide film thickness at which C_H will just attain C_{HS} at $t = \infty$) is given by :-

$$d_{crit} = \frac{D_o \cdot C_1 \cdot r}{D_M \cdot C_{HS}} \tag{10}$$

For example, referring to Figure 5, if C_{HS} is about 0.1 C_1 then hydride attack would never be initiated at any location where the oxide film thickness is greater than about 30 nm. As the temperature changes then D_o, D_M, C_1 and C_{HS} would all be expected to

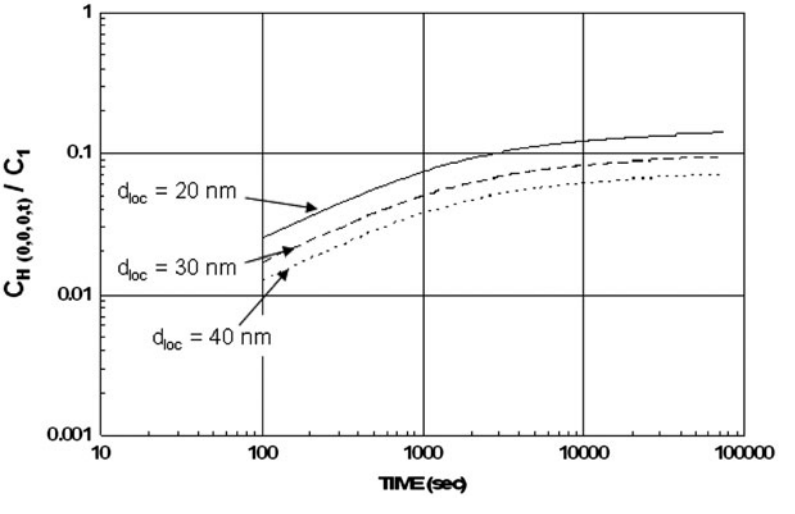

Figure 5. Time dependence of the calculated hydrogen concentration in the metal just at the oxide–metal interface (i.e. $z = 0$) for 3 different values of local oxide film thickness (and for $D_M = 5 \times 10^{-10}$ cm^2 s^{-1}, $D_o = 10^{-13}$ cm^2 s^{-1} and $r = 15$ μm).

vary and so d_{crit} could also be expected to vary. However, any change in hydrogen pressure would only affect C_1, and so, d_{crit} would vary in sympathy with this pressure. The value of C_1 may not necessarily be directly proportional to the applied hydrogen pressure (in fact we later see that a comparison of this model with a limited experimental data set implies that C_1 varies as the square root of hydrogen pressure) but Equation (10) implies that d_{crit} varies directly as C_1; consequently, any reduction in hydrogen pressure (or C_1) would reduce d_{crit} and so, assuming we had some oxide film thickness distribution over the entire surface, render more of the surface less prone to hydride attack. So, according to this model (as expressed by Equation (7)), two conditions are required for hydride attack to occur in the metal beneath the oxide film at any location; firstly, the magnitude of C_1 must be greater than C_{HS} (as it is the concentration difference across the oxide film, $C_1 - C_{H(0,0,0,t)}$, which drives hydrogen to flow across the oxide and $C_{H(0,0,0,t)}$ can only attain the value of C_{HS} if $C_1 > C_{HS}$) and, secondly, d_{loc} must be less than d_{crit} or, referring to Equation (10), C_1 must be greater than $d_{loc}.D_M.C_{HS}/D_o.r$.

Further exploring the characteristics of this hydride initiation model, it may be shown that the model is compatible with the observation that, whereas many hydride sites grow rapidly after their initiation and soon disrupt the overlying oxide film, some hydride sites cease their growth after attaining some small size and may never disrupt the oxide film. This phenomenon may be explained in terms of the parameter d_{crit}, and how the magnitude of d_{loc} compares with the magnitude of d_{crit}. Firstly, for the thinnest regions of oxide film where $d_{loc} << d_{crit}$, both the initial hydrogen flow (per unit area) across the oxide–metal interface into the metal ($C_1.D_o/d_{loc}$) and the rate of increase in

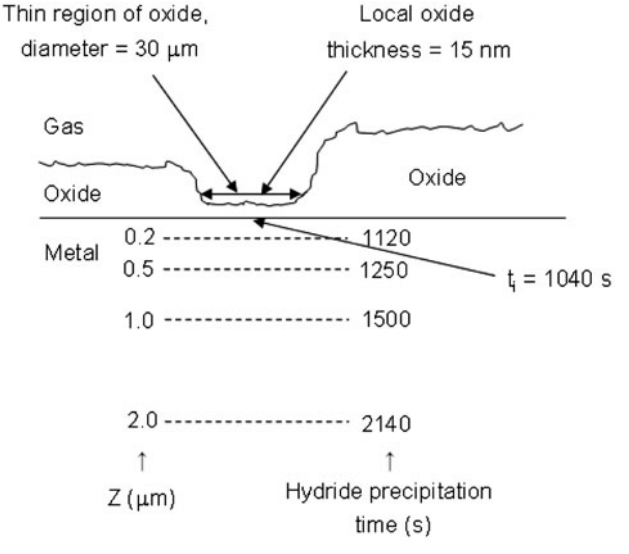

Figure 6a. Diagram showing the calculated times at which the hydride precipitation front reaches a particular depth (z) beneath the oxide–metal interface. In this case, the oxide film thickness, 15 nm, is somewhat less than d_{crit}, 30 nm, and so, the advance of the precipitation front is quite rapid after the initiation of the first hydride, at $z = 0$, which occurs after 1.040×10^3 s (for $C_{HS}/C_I = 0.1$, $D_M = 5 \times 10^{-10}$ cm^2 s^{-1}, $D_o = 10^{-13}$ cm^2 s^{-1} and $r = 15$ μm).

Downloaded by [The University of Manchester Library] at 03:21 22 September 2017

Downloaded by [The University of Manchester Library] at 03:21 22 September 2017

hydrogen concentration in the metal just below this interface (Equation (9)) are greatest. Consequently, at any location where the oxide film is very thin, the hydrogen solubility of the metal will be exceeded first just beneath the oxide–metal interface at the centre of that oxide area element (i.e. at $x = y = z = 0$). Also, as the rate of increase in hydrogen concentration at any depth, z, beneath this interface is also large then the boundary of the region beneath the oxide–metal interface in which the hydrogen solubility is exceeded and hydride is precipitated advances rapidly. Making use of Equation (6) in an example calculation, Figure 6(a) shows the time to precipitate hydride at various depths beneath the centre of a locally thin region of oxide film where the local oxide film thickness is significantly less than d_{crit}. Consequently, in this case, after only a relatively short time the metal will have been converted to hydride to a considerable depth (compared to the oxide thickness) and the resulting volume expansion would be expected to readily disrupt the overlying oxide film; the growth of this hydride site thereafter would not be controlled by hydrogen diffusion through the overlying oxide film. For regions of oxide film where d_{loc} is only marginally less than d_{crit}, however, the hydrogen concentration in the metal just beneath the oxide–metal interface approaches C_{HS} only slowly (see Figure 6(b) where d_{loc} has the value of 87% d_{crit}) and, at only a short distance into the metal, the time for C_H to attain the value of C_{HS} and precipitate hydride may approach infinity (according to Equation (6)). Consequently, in this case where d_{loc} is only marginally less than d_{crit}, hydride may be precipitated in the metal just beneath the oxide film but the infinitesimally slow growth of the site may be such that the hydride-metal reaction front advances only a very small distance into the metal in an exceedingly long time (i.e. perhaps longer than any typical

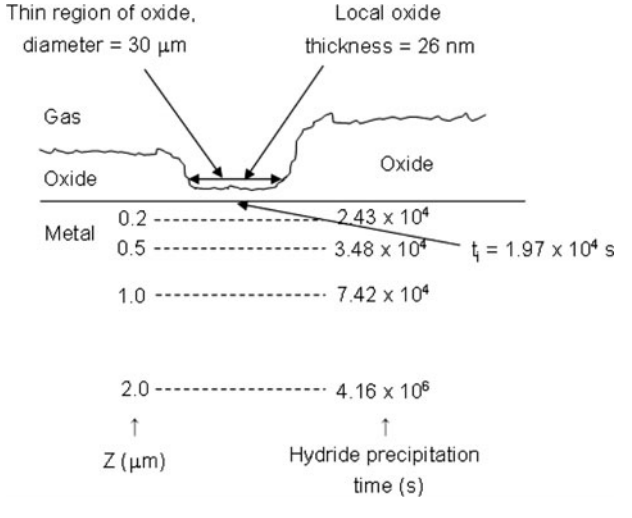

Figure 6b. Diagram showing the calculated times at which the hydride precipitation front reaches a particular depth (z) beneath the oxide–metal interface. As the oxide film thickness, 26 nm, is within a few % of d_{crit}, 30 nm, the rate of advance of the precipitation front is very slow after the initiation of the first hydride, at $z = 0$, which occurs after 1.97×10^4 s (for $C_{HS}/C_1 = 0.1$, $D_M = 5 \times 10^{-10}$ cm^2 s^{-1}, $D_o = 10^{-13}$ cm^2 s^{-1} and $r = 15$ µm). Furthermore, the rate of advance of the precipitation front continually decreases with time becoming virtually zero after it reaches a depth of 1 µm or so.

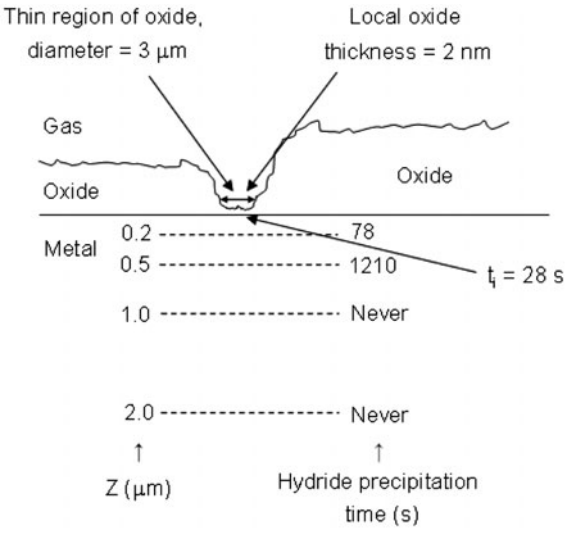

Figure 6c. Diagram showing the calculated times at which the hydride precipitation front reaches a particular depth (z) beneath the oxide–metal interface. As the diameter of the locally thin region of oxide film is now much reduced in this example, together with the fact that the value of the local oxide film thickness, 2 nm, is 67% of that of d_{crit} (3 nm), then hydride is initiated just beneath the oxide–metal interface in only a short time, 28 s, but little further growth of this hydride site beyond a depth of about 0.5 μm or so occurs (for $C_{HS}/C_1 = 0.1$, $D_M = 5 \times 10^{-10}$ cm^2 s^{-1}, $D_o = 10^{-13}$ cm^2 s^{-1} and $r = 1.5$ μm).

experiment). Consequently, the volume of hydride generated may never be sufficient to disrupt the overlying oxide and the depth-wise growth of that hydride site virtually ceases, being asymptotic to some final size. Thus, after its formation beneath the oxide film, the hydride site would appear to grow only marginally before apparently being terminated. Such observations of the arrested growth of hydride sites beneath the surface oxide film have been reported by Owen and Scudamore [3] and Arkush [4] for uranium hydriding and by Benamar et al. [20] for the hydriding of gadolinium. However, these authors also reported that, where the growths of some hydride sites were arrested after some time, those sites also had short initiation times. This observation would appear to be incompatible with the examples given in Figures 6(a) and 6(b). However, it was shown above that the value of $C_{H(0,0,0,t)}$ approximates to $D_o.C_1.r/d_{loc}.D_M$ as the value of $(r/(2(D_M\ t)^{½})$ approaches zero, and this condition occurs not only as t approaches infinity but also as r approaches zero. This means that, even for quite short times, the value of $C_{H(0,0,0,t)}$ approximates to $D_o.C_1.r/d_{loc}.D_M$ as r approaches zero; this characteristic of Equation (7) therefore means that $C_{H(0,0,0,t)}$ rapidly attains its equilibrium value as r tends to zero, and even if d_{loc} is close to d_{crit}. Consequently, if r is small and d_{loc} is not considerably less than d_{crit} then this would be compatible with hydride sites being initiated at quite short times but with their growth then being terminated not long thereafter; this situation is illustrated by the example shown in Figure 6(c) where the hydride site is initiated in a time of less than 100 s but the value of $C_{H(0,0,z,t)}$ never attains the value of C_{HS} even at a depth of just 1 μm beneath the centre of this locally thin region of oxide film.

Downloaded by [The University of Manchester Library] at 03:21 22 September 2017

Downloaded by [The University of Manchester Library] at 03:21 22 September 2017

Although the concept of d_{crit} is useful in indicating quantitatively how protective a given locally thin region of oxide film may be, its derivation (Equation (10)) is based on Equation (7) describing the time dependence of the hydrogen concentration in the metal following hydrogen diffusion through that locally thin region of oxide (and through that region of oxide only). Consequently, this expression could be criticized on the grounds that there will also be some further contribution to this hydrogen concentration resulting from hydrogen flow through the thicker neighbouring oxide. We can quantify this extra contribution to $C_{H(0,0,z,t)}$ beneath our considered thin region of oxide with reference to our earlier derivation of $C_{H(0,0,z,t)}$. Thus, referring to Equation (2) for the hydrogen concentration beneath our locally thin region of oxide for an instantaneous mass of hydrogen (m_a per unit area) deposited at time $t = 0$ over the circular area of radius r centred at (0, 0, 0), we can immediately write down an expression for the hydrogen concentration at (0, 0, z, t) at any time t due to mass m_b of hydrogen (per unit area) deposited instantaneously at time $t = 0$ over the remaining surface (i.e. from $a = r$ to $a = \infty$) at time $t = 0$ as:

$$C_{H(0,0,z,t)} = \frac{m_b}{4(\pi D_M t)^{3/2}} \int_0^{2\pi} \int_r^{\infty} a\mathrm{Exp}\left[-\frac{(a^2+z^2)}{4D_M t}\right] da d\theta \tag{11}$$

Except for the integration limits, this is the same integration solved earlier, and so, it can be seen that this expression integrates to:

$$C_{H(0,0,z,t)} = \frac{m_b \mathrm{Exp}\left[-\frac{r^2+z^2}{4D_M t}\right]}{(\pi D_M t)^{1/2}}$$

If we now consider a continuous source (from $a = r$ to $a = \infty$ for all θ) which emits mass $dt' \cdot m'_b$ g cm^{-2} during any finite time interval from $t = t'$ to $t = t' + \delta t'$ from time $t = 0$ then the contribution at any point $(0, 0, z)$ at time t is just the integral of this expression or:

$$I_3 = \frac{m'_b}{(\pi D_M)^{1/2}} \int_0^t \frac{1}{(t-t')^{1/2}} \mathrm{Exp}\left[-\frac{r^2+z^2}{4D_M(t-t')}\right] dt'$$

Apart from a minus sign, this integration is the same as an integral solved earlier and is:

$$I_3 = \frac{2m'_b(t)^{1/2}}{(D_M)^{1/2}} \left[i\mathrm{Erfc}\left[\frac{(r^2+z^2)^{1/2}}{(4D_M t)^{1/2})}\right]\right]$$

Finally, if we replace m'_b by $C_1 \cdot D_o/d_o$, that is, the near-constant flow of hydrogen through all of the oxide (to which we assign the average thickness, d_o, of the total surface oxide film) neighbouring our considered individual localized thin area of oxide then our previous expression (Equation (6)) for the hydrogen concentration $C_{H(0,0,z,t)}$ beneath our considered thin oxide area now becomes:

$$C_{H(0,0,z,t)} = \frac{2C_1 D_o(t)^{1/2}}{d_{loc}(D_M)^{1/2}}\left[i\mathrm{Erfc}\left[\frac{z}{(4D_M t)^{1/2}}\right] - i\mathrm{Erfc}\left[\frac{(r^2+z^2)^{1/2}}{(4D_M t)^{1/2}}\right]\right] + \frac{2C_1 D_o(t)^{1/2}}{d_o(D_M)^{1/2}}\left[i\mathrm{Erfc}\left[\frac{(r^2+z^2)^{1/2}}{(4D_M t)^{1/2}}\right]\right] \quad (12)$$

In theory, this extra contribution to the hydrogen concentration beneath a thin region of oxide due to hydrogen flow through thicker neighbouring oxide would mean that, even if our considered thin region of oxide had a thickness slightly greater than d_{crit}, hydride would eventually be precipitated beneath it. However, in practice, the extra hydrogen flow through neighbouring oxide could be so small that the concept of d_{crit} would still be meaningful.

Although most studies report hydride sites (not associated with inclusions) being initiated in the metal at the oxide–metal interface [3,4,10], some have presented evidence of blisters of expanded metal clearly indicative of sub-surface hydride formation [11]. It is suggested here that this difference in the depth-wise location of hydride site initiation is associated with the non-isotropic nature of the metal, which can develop due to the work hardening of near-surface layers resulting from mechanical polishing. Firstly, for isotropic metal and therefore uniform spatial hydrogen solubility, this model predicts that hydride initiation should always occur in the metal just at the oxide–metal interface (see Figure 4). However, abrasive polishing (rather than electropolishing) would be expected to generate a much more defective metal lattice, and this would be associated with a significant increase in hydrogen solubility [18]. However, although the increased density of lattice defects could easily be understood to significantly increase hydrogen solubility, only a minimal change in hydrogen diffusion coefficient may be anticipated. If the near-surface hydrogen solubility in the metal is much greater than that at sub-surface regions, therefore, then this model readily predicts that hydride attack should first initiate at or very near the interface between the two distinct regions of hydrogen solubility. Based on the premise that any degree of near-surface work hardening would not substantially modify the diffusion coefficient of hydrogen in the metal, the time and spatial dependence of the hydrogen concentration in the metal beneath our locally thin region of oxide film would be the same as for the totally isotropic metal and given by Equation (6). However, despite the fact that the hydrogen concentration in

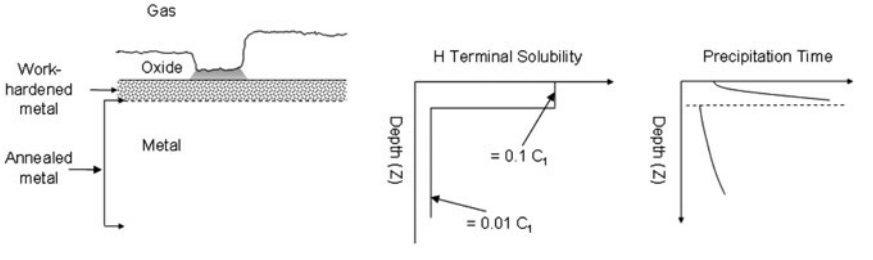

Figure 7. Illustration of how near-surface work-hardened layer of metal developed during mechanical polishing, and a presumed corresponding depth-wise variation in terminal hydrogen solubility, may lead to the initial sub-surface precipitation of hydride (as calculated using Equation (6)).

Downloaded by [The University of Manchester Library] at 03:21 22 September 2017

Table 1. Data to illustrate the phenomenon of sub-surface precipitation. In this example data, it is assumed that the H solubility in the near-surface regions of the metal (from 0 to 10 μm) is 10 times greater than that of the underlying metal due to previous surface polishing. The time for $C_{H(0,0,z,t)}$ at any depth in the metal to attain the value of the local H solubility limit is then calculated according to Equation (6) ($D_M = 5 \times 10^{-10}$ cm^2 s^{-1}, $D_o = 10^{-13}$ cm^2 s^{-1}, $d_{loc} = 20$ nm and $r = 15$ μm).

Depth Z (μm)	C_{HS}/C_1	Time for $C_{H(0,0,z,t)}$ to reach value of C_{HS} (s)
0	0.1	2.90×10^3
2	0.1	7.90×10^3
4	0.1	3.43×10^4
6	0.1	3.30×10^6
8	0.1	Never
10	0.01	7.8×10^2
12	0.01	1.07×10^3
14	0.01	1.43×10^3
16	0.01	1.87×10^3
18	0.01	2.41×10^3
20	0.01	3.07×10^3

the metal increases more rapidly in the near-surface regions (i.e. low z values) than deeper within the metal, a substantial increase in near-surface hydrogen solubility could mean that hydride is first precipitated at some depth below the oxide–metal interface in the un-work-hardened metal which has a substantially lower hydrogen terminal solubility. Figure 7 illustrates this situation in graphical form with associated theoretical data given in Table 1. Thus, for the assumed depth-wise differences in hydrogen solubility, the data show that hydride is precipitated first not at the oxide–metal interface in the work-hardened metal, where hydride precipitation is calculated to occur after a time of 2.9×10^3 s, but 10 μm beneath the oxide–metal interface just within the annealed metal after a time of only 7.8×10^2 s. Furthermore, the data show that, having precipitated first at a depth of 10 μm beneath the oxide–metal interface after only 7.8×10^2 s, from this depth the hydride precipitation front then continues to extend downwards into the metal for more than 2×10^3 s, to a depth of almost 20 μm, before hydride is eventually precipitated in the metal at the oxide–metal interface after a time of 2.9×10^3 s.

3.2. *Hydride attack pattern over entire coupon surface*

Having derived an expression for the time dependence of the hydrogen concentration in the metal beneath any thin region of oxide film we may calculate the times at which hydride sites are initiated over all regions of any surface if we define the thickness distribution of the oxide film. If oxidation of a polycrystalline sample of the metal (prior to any hydrogen exposure) occurs at different rates on the surfaces of the differently orientated metal grains, the developed surface oxide film may perhaps possess a Gaussian thickness distribution. In this case, the number of oxide area elements $N(d_{loc})$ having a thickness between d_{loc} and $d_{loc} + \delta d_{loc}$ is given by :-

Downloaded by [The University of Manchester Library] at 03:21 22 September 2017

$$N(d_{loc}) = \frac{AM}{\sigma(2\pi)^{1/2}} \mathrm{Exp}\left[-\frac{(d_{loc}-d_o)^2}{2\sigma^2}\right]\delta(d_{loc}) \tag{13}$$

where d_o is the mean oxide film thickness, σ is the standard deviation of the Gaussian oxide thickness distribution and the product $A.M$ is the total number of oxide area elements (each radius r) over the entire sample surface (where A is the total sample area and M is equal to $1/\pi r^2$). Next, we define the parameter, d_s, to be that value of local oxide film thickness for which hydride is just being precipitated in the metal beneath that small area of oxide (at $z = 0$) at any time, t. Therefore, from Equation (7) (i.e. ignoring the lesser flow through neighbouring thicker oxide) and noting that the value of $C_{H(0,0,0,t)} = C_{HS}$ just at precipitation then d_s is given by:

$$d_s = \frac{2\ C_1 D_o(t)^{1/2}}{C_{HS}(D_M)^{1/2}}\left[\frac{1}{(\pi)^{1/2}} - i\mathrm{Erfc}\left[\frac{r}{(4D_M t)^{1/2}}\right]\right] \tag{14}$$

Therefore, the number of hydride sites (N_t) initiated from time zero to time, t, is just equal to the number of oxide area elements having a thickness less than or equal to d_s and is given by:

$$N(t) = \int_0^{d_s} \frac{AM}{\sigma(2\pi)^{1/2}} \mathrm{Exp}\left[-\frac{(d_{loc}-d_o)^2}{2\sigma^2}\right] d(d_{loc})$$

Making the substitution $\Phi = (d_{loc} - d_o)/\sigma\sqrt{2}$, this integral may be solved to give:

$$N(t) = \frac{AM}{2}\left[\mathrm{Erf}\left(\frac{d_s - d_o}{\sigma(2)^{1/2}}\right) + \mathrm{Erf}\left(\frac{d_o}{\sigma(2)^{1/2}}\right)\right]$$

Finally, replacing the term d_s with fundamental parameters (see Equation (14)) gives:

$$N_t = \frac{AM}{2}\left[\mathrm{Erf}\left(\frac{\left(\frac{2C_1 D_o(t)^{1/2}}{C_{HS}(D_M)^{1/2}}\left[\frac{1}{(\pi)^{1/2}} - i\mathrm{Erfc}\left[\frac{r}{(4D_M t)^{1/2}}\right]\right]\right) - d_o}{\sigma(2)^{1/2}}\right) + \mathrm{Erf}\left(\frac{d_o}{\sigma(2)^{1/2}}\right)\right] \tag{15}$$

4. Model comparison with experimental observations

A full quantitative comparison of this model with experimental uranium hydriding data is beyond the scope of this paper, but a later paper [13] will compare the form of Equation (15) for N_t with experimental data at various temperatures and hydrogen pressures. Here, however, a limited and mainly qualitative comparison of the model with reported uranium hydriding data is given to illustrate further how this model may explain a number of experimental observations.

Referring to Equation (8), we may write the approximate expression for precipitation just beneath a thin region of oxide, thickness $d_{\min}$, as:

Downloaded by [The University of Manchester Library] at 03:21 22 September 2017

$$C_{HS} \approx \frac{2C_1 D_o (t_i)^{1/2}}{d_{\min}(\pi D_M)^{1/2}} \tag{16}$$

Here, $d_{\min}$ refers to the thinnest value of oxide film thickness over the entire sample surface, and t_i is therefore the induction time (i.e. the time to the initiation of the first hydride site). In this qualitative comparison of the model with experimental data, it is not necessary to define the value of $d_{\min}$ in terms of any supposed oxide film thickness distribution, but we may use Equation (16) to compare the temperature and pressure dependence of the induction time for experiments where samples have been prepared by some standard method such that $d_{\min}$ might be expected to be unchanged from experiment to experiment. So, provided that the measured induction time, t_i, is $>> (d_{\min})^2/6D_o$, such that our assumption of constant flow through that region of the oxide for all times up to t_i (a founding assumption of Equation (8)) is credible, and provided also that $t_i << r^2/4D_M$ such that the value of $i\mathrm{Erfc}(r/(4D_M t_i)^{1/2})$ is much less than $1/(\pi)^{1/2}$ then we can write from Equation (16):

$$\text{Induction Time} \approx \frac{\pi D_M (C_{HS} d_{\min})^2}{4(C_1 D_o)^2} \tag{17}$$

This expression suggests that for uranium hydriding experiments using coupons bearing oxide films having reproducible characteristics such that $d_{\min}$ is the same on the different coupons, the measured induction time should vary as the inverse of the square of C_1. Now, reported experimental data [5] indicate that the induction time for uranium hydriding experiments at constant temperature varies approximately as the inverse of the hydrogen pressure. Thus, the model is compatible with this reported pressure variation if we assume that C_1 is proportional to the square root of the applied hydrogen pressure. This is a reasonable expectation and compatible with the idea that the diffusing hydrogen species in uranium dioxide are atomic [16] rather than molecular. Furthermore, if hydrogen dissociation on the oxide surface is the first step leading to the initiation of any hydride site, then this conclusion is also compatible with the observation that gaseous impurities may extend hydride induction times [21] if such impurities preferentially adsorb on the oxide surface and so limit the degree of hydrogen dissociation and reduce the magnitude of C_1.

Lastly, we may consider the temperature variation of the induction time for uranium hydriding, which is reported to exhibit a composite activation energy of about 58 kJ mol^{-1} [22]. According to Equation (17), the inverse of the induction time is approximately proportional to $(D_o \cdot C_1/C_{HS})^2/D_M$, and so we can test the compatibility of Equation (17) with the reported data by considering the temperature dependencies of C_{HS}, D_M, D_o and C_1. Firstly, data from the studies of Wheeler [14] and Aratono et al. [15] suggest that D_o increases with temperature with an activation energy in the region of 60 to 76 kJ mol^{-1}. Also, data from Mallett and Trzeciak [23] suggest that D_M increases with temperature with an activation energy of about 46 kJ mol^{-1} whilst the terminal solubility of hydrogen in the metal, C_{HS}, also increases with temperature with an activation energy of about 52 kJ mol^{-1}. Data concerning the temperature variation of the hydrogen solubility in uranium dioxide are sparse and more difficult to interpret due to the fact that there appears to be more than one lattice site which can be occupied by the dissolving hydrogen [16]. For the nominally stoichiometric oxide, however,

Downloaded by [The University of Manchester Library] at 03:21 22 September 2017

Sherman and Olander found that the deduced activation energies describing the temperature variations of the measured solubilities for the two identified bound states were 53 and 121 kJ mol^{-1}. It is anticipated that only the bound state associated with the lowest of these two activation energies (i.e. 53 kJ mol^{-1}) is likely to be accessible to hydrogen species during low-temperature hydriding experiments. Therefore, referring again to Equation (17) and to these reported activation energies for D_M, D_o, C_{HS} and C_1, the expected activation energy describing the temperature variation of the inverse of the induction time for uranium hydriding experiments conducted at reasonably low temperatures is either $((2 \times 60) + (2 \times 53)) - ((2 \times 52) + 46) = 76$ kJ mol^{-1} using the value of D_o as reported by Wheeler [14] or $((2 \times 76) + (2 \times 53)) - ((2 \times 52) + 46) = 108$ kJ mol^{-1} using the value of D_o as reported by Aratono et al. [15]. Thus, considering the large uncertainties in some of the cited activation energies, the calculated value of 76 kJ mol^{-1} compares reasonably well with the value observed experimentally (58 kJ mol^{-1} [22]) for uranium hydriding studies conducted at temperatures within the range 30–125 °C.

5. Summary

A model for the initiation of hydride sites on uranium metal has been described for conditions of constant hydrogen pressure. It is proposed that thin areas of surface oxide favour enhanced hydrogen permeation through the oxide and lead to the more rapid initiation of hydride sites. By assuming that conditions of near-constant flow of hydrogen species are attained through such thin oxide areas in a relatively short time, the time and spatial dependence of the hydrogen concentration field in the underlying metal has been calculated. Presuming that hydride is precipitated at any location in the metal once the hydrogen concentration attains the terminal solubility limit of the metal at the prevalent temperature, the time to precipitate hydride has been calculated in terms of this terminal hydrogen solubility and other relevant oxide and metal properties. It has been shown that the model is reasonably compatible with the reported temperature and pressure dependence of the hydride induction time. Although the model predicts that, for isotropic metal with uniform hydrogen solubility, hydride reaction sites are precipitated in the metal just adjacent to the oxide–metal interface, it has been shown how non-uniform metal hydrogen solubility introduced by mechanical polishing may lead to sub-surface precipitation of hydride. The model can also explain the arrested growth of certain hydride sites initiated beneath the oxide film in terms of a model parameter, d_{crit}. Thus, this model can account for at least two families of hydride sites identified in previous studies [3,4] – (i) hydride sites which initiate rapidly beneath the oxide after the initial exposure of the sample to hydrogen but which then grow only marginally or not at all thereafter (associated with low values of r and for which $d_{loc} < d_{crit}$) (ii) hydride sites associated with other but larger thin areas of oxide (but for which d_{loc} is still $< d_{crit}$) which grow continually until the overlying oxide is disrupted and after which free growth ensues. Lastly, having derived an expression for the hydride initiation time at any location in terms of the magnitude of the local oxide film thickness, a further expression has been derived for the number of hydride sites initiated on an entire sample surface in any given time, N_t, by assuming a Gaussian oxide film thickness distribution over the entire sample surface.

Downloaded by [The University of Manchester Library] at 03:21 22 September 2017

It may be noted that the described model may well be applicable to other metal–oxide–hydrogen systems provided that the stated model assumptions remain valid. Metals (or dilute alloys of metals) which form a hydride and which generally form a micro-crystalline, single-phase surface oxide film which exhibits differential growth on differently orientated metal grains would be potentially suitable. Additionally, the diffusion coefficient of hydrogen in the metal should be somewhat greater than that in the surface oxide film. On this basis, the model may be applicable to the hydriding behaviour of the pure metals Ni, Zr and Hf and dilute alloys of these metals. Potentially, it is even possible that the model may be applied also to corrosion phenomena other than hydriding.

Downloaded by [The University of Manchester Library] at 03:21 22 September 2017

Acknowledgement

The author thanks Dr. P. Morrall for helpful comments and review of this document.

References

[1] R.K. Schulze, *Private Communication*, Los Alamos National Laboratory, Los Alamos, NM, 2004.
[2] G.C. Allen and J.C.H. Stevens, J. Chem. Soc., Faraday Trans. 1 (1988) p.165.
[3] L.W. Owen and R.A. Scudamore, Corr. Sci. 6 (1966) p.46.
[4] R. Arkush, A. Venkert, M. Aizenshtein, S. Zalkind, D. Moreno, M. Brill, M.H. Mintz and N. Shamir, J. Alloys Compd. 244 (1996) p.197.
[5] J. Glascott, AWE Discovery 6 (2003) p.16.
[6] D. Cohen, Y. Zeiri and M.H. Mintz, J. Alloys Compd. 184 (1992) p.11.
[7] D.F. Teter, R.J. Hanrahan and C.J. Wetteland, LANL Report LA-UR 00-4514, 2000.
[8] F.W. Young, J.V. Cathcart and A.T. Gwathmey, Acta Metall. 4 (1956) p.145.
[9] J.V. Cathcart, G.F. Peterson and C.J.J. Sparks, J. Electrochem. Soc. 116 (1969) p.664.
[10] T. Scott, G.C. Allen, I.M. Findlay and J. Glascott, Phil. Mag. 87 (2007) p.177.
[11] J.F. Bingert, R.J. Hanrahan, R.D. Field and P.O. Dickerson, J. Alloys Compd. 365 (2004) p.138.
[12] J. Glascott, Philos. Mag. submitted for publication.
[13] J. Glascott, J. Petherbridge and S. Bazley. In preparation.
[14] V.J. Wheeler, J. Nuc. Mat. 40 (1971) p.189.
[15] Y. Aratono, M. Nakashima, M. Saeki and E. Tachikawa, J. Nuc. Mat. 110 (1982) p.201.
[16] D.F. Sherman and D.R. Olander, J. Nuc. Mat. 166 (1989) p.307.
[17] J. Crank, *The Mathematics of Diffusion*, 2nd ed., Oxford University Press, Oxford, 1975.
[18] C.D. Taylor, T. Lookman and R.S. Lillard, Acta Mater. 58 (2010) p.1045.
[19] H.S. Carslaw and J.C. Jaeger, *Conduction of Heat in Solids*, 2nd ed., Clarendon Press, Oxford, 1959.
[20] G. Benamar, D. Schweke, J. Bloch, T. Livneh and M.H. Mintz, J. Alloys Compd. 477 (2009) p.188.
[21] J. Bloch, D. Brami, A. Krenmer and M.H. Mintz, J. Less-Common Met. 139 (1986) p.371.
[22] S. Bazley, J. Petherbridge and J. Glascott, Solid State Ionics 211 (2012) p.1.
[23] M.W. Mallett and M.J. Trzeciak, Trans. A.S.M 50 (1957) p.981.